Theory of self-diffusion in alkali metals: I. Results for monovacancies in Li, Na, and K

2000 J. Phys.: Condens. Matter 12 1171

(http://iopscience.iop.org/0953-8984/12/7/303)

J. Phys.: Condens. Matter **12** (2000) 1171–1194. Printed in the UK PII: S0953-8984(00)07388-4

Theory of self-diffusion in alkali metals: I. Results for monovacancies in Li, Na, and K

V Schott†‡, M Fähnle†‡ and P A Madden§

† Max-Planck-Institut für Metallforschung, Heisenbergstraße 1, D-70569 Stuttgart, Germany
‡ Institut für Theoretische und Angewandte Physik, Universität Stuttgart, Pfaffenwaldring 57, D-70569 Stuttgart, Germany
§ Physical Chemistry Laboratory, South Parks Road, Oxford OX1 3QZ, UK

Received 2 September 1999, in final form 13 December 1999

Abstract. The phonon dispersion curves for perfect crystals of bcc Li, Na, and K are calculated by the *ab initio* force-constant method in a supercell approach. It is shown that the coupling constants of Li decay much more slowly in space than those for Na and K, so for Li the phonon spectrum could not be reliably determined with the supercell sizes used in the calculations. From the phonon spectra of the perfect supercell and the supercell with a monovacancy the vacancy formation entropy is calculated for Na (1.36 k_B) and K (0.78 k_B). Furthermore, the formation energy (0.53, 0.34, and 0.30 eV) and the formation volume (about 0.5 Ω_0) are obtained for Li, Na, and K, and the temperature and pressure dependences of the formation entropy and volume are investigated for the case of Na; a strong decrease of the formation volume with increasing pressure is found. The migration energies and volumes are determined within the framework of the transition-state theory. The migration energies are small (about 0.05 eV) for Li, Na, and K, and the migration volumes are small and negative for Li and Na. The calculated activation energies for self-diffusion (0.58, 0.39, and 0.35 eV) agree well with experimental data. Neglecting the migration entropy and inserting Flynn's *ansatz* for the attempt frequency, the absolute values of the self-diffusion coefficients are determined as a function of temperature. For Na these values agree well with experimental data, whereas for K the calculated values are too small except for low temperatures.

1. Introduction

In the present paper we report on the results of our calculations of the properties of monovacancies (1V) in the bcc phases of the alkali metals Li, Na, and K.

It is widely accepted that monovacancies play an important role for self-diffusion in bcc Li and Na, for the following reasons:

(1) Simultaneous measurements of the macroscopic thermal expansion and lattice parameters have shown [1–3] that vacancies and not self-interstitials are the dominant intrinsic atomic defects in thermal equilibrium. A strong contribution of self-interstitials could be excluded also by the *ab initio* electron theory [4, 5] due to the high formation energies.
(2) The data from quasielastic neutron scattering experiments for Na [6] could be consistently interpreted in terms of a random migration of vacancies and divacancies.
(3) For Li the activation energy of self-diffusion via monovacancies as obtained by the transition-state theory and the *ab initio* electron theory [7] is in very good agreement with experimental activation energies for self-diffusion obtained by mass spectroscopy [8] or NMR experiments [9]. For Na the *ab initio* result [10] agreed very well with the smallest

0953-8984/00/071171+24$30.00

activation energy obtained by fitting the data from NMR experiments [11] or radiotracer experiments [12] with two or three exponentials.

On the other hand, there are some peculiarities of self-diffusion in Li and Na which are still under discussion:

(i) Most recently it was found by an elastic-recoil-detection analysis for Li [13] and by radiotracer experiments after ^{24}Na implantation for Na [14] that at very low temperatures the diffusion coefficients are larger than those which would arise if the data for high temperatures were extrapolated to low temperatures. It was argued [13, 14] that this enhancement of the self-diffusion is related to the low-temperature martensitic transformation of Li and Na. Corresponding experiments on K would be very interesting because this material does not exhibit a martensitic transformation.

(ii) Inserting for Na the experimental values for H^{SD} and H^{f} yields a very small value for the migration enthalpy H^{m} of the order of $2k_{\mathrm{B}}T_{\mathrm{m}}$, where T_{m} is the melting temperature. Similar small values for $E^{\mathrm{m}}_{1\mathrm{V}}/2k_{\mathrm{B}}T_{\mathrm{m}}$ were found within the framework of the transition-state theory and the *ab initio* calculations for monovacancies in Li [7, 10] and Na [10]. It may be argued [15] that for such low values of $E^{\mathrm{m}}_{1\mathrm{V}}/2k_{\mathrm{B}}T_{\mathrm{m}}$ the notion of discrete vacancy jumps is no longer valid and that therefore the transition-state theory of self-diffusion [16] cannot be applied. To check the validity of the transition-state theory for the case of Na, the migration energy of monovacancies as deduced from the transition-state theory was compared with the migration energy obtained from a molecular dynamics calculation of mean square displacements based on volume-dependent pair potentials [17]. A good agreement was found, but this does not necessarily mean that the transition-state theory can be applied also for a calculation of the whole self-diffusion coefficient $D(T)$, especially its absolute value.

(iii) The kinetic energy factor ΔK obtained experimentally [12] from the isotope effect parameter is rather low for the case of Na, and it was argued [15] that this is not easy to understand if a monovacancy mechanism were to be assumed but that it would naturally arise for a mechanism of self-diffusion by direct exchange of neighbouring atoms. However, such a mechanism could be excluded by *ab initio* calculations [10, 18] which yielded activation energies for the direct exchange in Li and Na which are about a factor of 3 larger than the experimental activation energies for self-diffusion. An explanation of the low value of ΔK in Na is thus still lacking.

(iv) The experimentally obtained activation volumes of Li [19] and Na [12] are smaller than half of the atomic volume Ω_0. Recent measurements of the NMR linewidth [20, 21] at room temperature and pressures up to 5 GPa gave hints of a strong decrease of the activation volumes with increasing pressure, arriving at values of (0.1–0.2) Ω_0 at the highest applied pressures. (It should be noted that these experiments are very difficult and that the analysis of these experiments is not on firm theoretical grounds [22]). It was argued [15] that such low values of the activation volumes are not expected for a monovacancy mechanism. *Ab initio* calculations of the activation volumes for Li and Na [18] within the framework of the transition-state theory yielded values which are indeed smaller than 0.5 Ω_0 and which are considerably reduced by a strong external pressure, but there were quantitative discrepancies between theory and experiment. These discrepancies may arise from problems related to the analysis of experimental data (see above) or from inappropriate assumptions of the theory. For instance, it is not clear whether the transition-state theory may be applied to Li and Na (see above and reference [18]). Furthermore, the calculations were performed for zero temperature. At finite temperature, contributions to the formation volume Ω^{f} and the migration volume Ω^{m} arising from the pressure

dependences of the formation and migration entropies may appear, which were neglected in the calculations of reference [18]).

(v) The temperature dependence of the diffusion constant deviates slightly but distinctly from an Arrhenius law at high temperatures, and it is tempting to explain this behaviour by a contribution of divacancies (2V) at high temperatures. This problem is considered in part II of the paper.

In the present paper we complete our former *ab initio* studies [4, 5, 7, 10, 17, 18] on the properties of monovacancies in the bcc phases of Li and Na and we extend them to the case of K, with special emphasis given to the calculation of formation entropies. These quantities are extremely difficult to calculate, and there are only a few examples in the literature where this problem was attacked by *ab initio* calculations [7, 23–25]. We have performed such calculations for Li [7], but unfortunately it turned out that there was an error in the analysis of the numerical data, and we have therefore redone the calculations for Li and extended them to Na and K. For Na we extended the calculations also to finite temperatures and determined the vacancy migration entropy and volume, therein taking into account the contribution to the migration volume from the pressure dependence of the migration entropy which was neglected in former calculations [18] (see point (iv)). The results for the self-diffusion coefficients are compared with experimental data.

2. Calculational procedure

2.1. Definition of the defect parameters

For a defect-mediated diffusion mechanism in a cubic crystal the tracer self-diffusion constant is given by (for a review, see reference [15])

$$D(T) = g f^{\mathrm{T}} c^{\mathrm{eq}} D_{\mathrm{defect}}. \tag{1}$$

Here the geometrical factor g and the correlation factor f^{T} are numerical factors which are well known for various defect mechanisms and which are assumed to be independent of T and p in the following, and D_{defect} denotes the diffusivity of the single defect. The concentration of defects in thermal equilibrium, c^{eq}, may be obtained from statistical mechanics, which yields for crystals with equivalent lattice sites the equation

$$c^{\mathrm{eq}} = \exp(-G^{\mathrm{f}}/k_{\mathrm{B}}T). \tag{2}$$

Here the free enthalpy of defect formation is given by

$$G^{\mathrm{f}} = H^{\mathrm{f}} - TS^{\mathrm{f}} = E^{\mathrm{f}} + p\Omega^{\mathrm{f}} - TS^{\mathrm{f}} \tag{3}$$

where H^{f}, E^{f}, S^{f}, and Ω^{f} are the enthalpy, energy, entropy, and volume of defect formation which describe the change in total enthalpy, energy, vibrational entropy, and volume of the crystal per created defect.

The diffusivity D_{defect} may be calculated within the framework of the transition-state theory [16] as long as the diffusion of the defect may be described as a random sequence of well-defined jumps, yielding

$$D_{\mathrm{defect}} = \nu_0 a_0^2 \exp(-G^{\mathrm{m}}/k_{\mathrm{B}}T). \tag{4}$$

Here ν_0 is the so-called attempt frequency and a_0 denotes the lattice constant. The free enthalpy of defect migration is given by

$$G^{\mathrm{m}} = H^{\mathrm{m}} - TS^{\mathrm{m}} = E^{\mathrm{m}} + p\Omega^{\mathrm{m}} - TS^{\mathrm{m}} \tag{5}$$

where H^{m}, E^{m}, S^{m}, and Ω^{m} are the enthalpy, energy, entropy, and volume of migration. The migration energy is thereby given by the energy difference between two static, fully relaxed configurations, the first one with the moving atom in the saddle-point configuration between the initial and the final state of the jump and the other with the atom in the initial potential minimum. The migration entropy S^{m} has to be obtained from the vibrational frequencies of the system in the initial state on the one hand and in the saddle point on the other hand, i.e., with the jumping atom confined to the ridge of the potential energy separating the initial and the final state of the jump. Thereby the motion of this atom along the coordinate responsible for the instability of the saddle point is frozen, and the corresponding normal frequency is replaced by the attempt frequency ν_0 which in the transition-state theory is an arbitrary frequency [16, 18, 26]. Flynn [26] has fixed ν_0 by making contact with the dynamical theory of diffusion, yielding $\nu_0 = \sqrt{3/5}\nu_{\mathrm{Debye}}$ where ν_{Debye} is the Debye frequency. The migration volume Ω^{m} is the difference in volume for the system on the one hand with the migrating atom in the static fully relaxed saddle-point configuration and on the other hand in the static fully relaxed initial configuration.

Combining equations (1)–(5) yields

$$D(T) = D_0 \exp\left(-\frac{E^{\mathrm{SD}} + p\Omega^{\mathrm{SD}}}{k_{\mathrm{B}}T}\right) \tag{6}$$

with

$$D_0 = f g^{\mathrm{T}} \nu_0 a_0^2 \exp\left(\frac{S^{\mathrm{SD}}}{k_{\mathrm{B}}}\right) \tag{7}$$

and $E^{\mathrm{SD}} = E^{\mathrm{f}} + E^{\mathrm{m}}$, $\Omega^{\mathrm{SD}} = \Omega^{\mathrm{f}} + \Omega^{\mathrm{m}}$, and $S^{\mathrm{SD}} = S^{\mathrm{f}} + S^{\mathrm{m}}$.

In the following we calculate the above-defined defect parameters for the case of monovacancies. We therein assumed (in accordance with the general belief) that $S^{\mathrm{m}}_{1\mathrm{V}}$ is close to zero, which is certainly the weakest point in our theory, and we insert Flynn's *ansatz* for ν_0. All the other quantities are calculated *ab initio*, i.e., without any adjustable parameter.

2.2. The supercell approach

The vacancy formation energy, entropy, and volume are calculated from $S^{\mathrm{f}}_{1\mathrm{V}} = -\partial G^{\mathrm{f}}_{1\mathrm{V}}/\partial T$, $\Omega^{\mathrm{f}}_{1\mathrm{V}} = \partial G^{\mathrm{f}}_{1\mathrm{V}}/\partial p$, and $E^{\mathrm{f}}_{1\mathrm{V}} = G^{\mathrm{f}}_{1\mathrm{V}} + TS^{\mathrm{f}}_{1\mathrm{V}} - p\Omega^{\mathrm{f}}_{1\mathrm{V}}$. For the calculation of $G^{\mathrm{f}}_{1\mathrm{V}}$ a supercell formalism is applied (for details, see reference [5]), i.e., large supercells containing N sites and one vacancy are arranged periodically. The quantity $G^{\mathrm{f}}_{1\mathrm{V}}$ then is determined from

$$G^{\mathrm{f}}_{1\mathrm{v}}(T, p) = G(N-1, 1, T, p) - G(N, 0, T, p) + \frac{1}{N}G(N, 0, T, p). \tag{8}$$

Here $G(N-1, 1, T, p)$ is the free enthalpy of the supercell containing $N-1$ atoms and one vacancy, whereas $G(N, 0, T, p)$ is the free enthalpy of a perfect supercell with N atoms. The free enthalpies G are obtained by minimizing the function

$$\tilde{G}(T, p; V) = F(T, V) + pV \tag{9}$$

with respect to the volume for fixed T and p. To do this, we calculate in the harmonic approximation the free energy

$$F(T, V) = E_0(V) + \frac{1}{2}\sum_{\lambda}\hbar\omega_{\lambda}(V) + k_{\mathrm{B}}T\sum_{\lambda}\ln(1 - \mathrm{e}^{-\hbar\omega_{\lambda}(V)/k_{\mathrm{B}}T}) \tag{10}$$

for various temperatures and volumes, fit Murnaghan's equation of state (see, for instance, reference [27]) to the data points, and use this equation of state for the minimization. In

equation (10) $E_0(V)$ represents the static energy of the supercell and the quantities ω_λ denote the phonon frequencies. Contributions to $F(T, V)$ originating from electronic excitations were neglected in our calculations. Indeed, we calculated the electronic contribution to the vacancy formation entropy according to reference [28] for Li and found an extremely small contribution only, in contrast to the behaviour of W [28].

The above-outlined procedure is very time consuming because it requires the *ab initio* calculation of $E_0(V)$ for the perfect lattice and for the supercell with a vacancy at various volumes (wherein the structural relaxation of the atoms around the vacancy has to be performed for each volume), and the *ab initio* calculation of the phonon frequencies ω_λ for the perfect lattice and for the structurally relaxed supercell with a vacancy at various volumes. Alternatively, we can calculate the free enthalpy $G_{1V}^{f}(T, p)$ of vacancy formation at given pressure p from the free energy $F_{1V}^{f,flc}$ of vacancy formation at fixed lattice constant according to [29]

$$G_{1V}^{f}(T, p) = F_{1V}^{f,flc} + p\Omega_0(T, p) \tag{11}$$

where Ω_0 is the atomic volume of the ideal crystal. In the following we assume that

$$\left.\frac{\partial S_{1v}^{f,flc}}{\partial \Omega_0}\right|_T = 0 \qquad \left.\frac{\partial E_{1V}^{f,flc}}{\partial T}\right|_{\Omega_0} = 0 \qquad \frac{\partial}{\partial T}\left(\beta_p \Omega_0 \left.\frac{\partial E_{1V}^{f,flc}}{\partial \Omega_0}\right|_T\right) = 0.$$

It will explicitly be shown that for the case of Na the first relation is nearly fulfilled (in contrast to the case for the behaviour of ionic crystals [30]), and it has explicitly been demonstrated in reference [4] that the second equation is approximately valid for the case of Li. With these assumptions the following relations may be obtained [4, 29, 31]:

$$\Omega_{1V}^{f}(T, p) = -\kappa_T \Omega_0 \left(\left.\frac{\partial E_{1V}^{f,flc}}{\partial \Omega_0}\right|_T + p\right) + \Omega_0 \tag{12}$$

$$E_{1V}^{f}(T, p) = E_{1V}^{f,flc}\big(a_0(T=0), T=0\big) - p\big(\Omega_{1V}^{f} - \Omega_0\big) \tag{13}$$

$$S_{1V}^{f}(T, p) = S_{1V}^{f,flc}\big(a_0(T=0), T\big) + \frac{\beta_p}{\kappa_T}\big(\Omega_{1V}^{f} - \Omega_0\big). \tag{14}$$

Here $a_0(T = 0)$ is the lattice constant at zero temperature, κ_T denotes the isothermal compressibility, and $E_{1V}^{f,flc}$ and $S_{1V}^{f,flc}$ are given by

$$E_{1V}^{f,flc} = E(N-1, 1, a_0) - E(N, 0, a_0) + \frac{1}{N}E(N, 0, a_0) - p(\Omega_{1V}^{f} - \Omega_0) \tag{15}$$

$$S_{1V}^{f,flc} = S(N-1, 1, a_0) - S(N, 0, a_0) + \frac{1}{N}S(N, 0, a_0) \tag{16}$$

$$S = -\frac{\partial F}{\partial T} = k_B \sum_\lambda \left\{ \frac{\hbar\omega_\lambda}{k_B T}\left[\exp\left(\frac{\hbar\omega_\lambda}{k_B T}\right) - 1\right]^{-1} - \ln\left[1 - \exp\left(-\frac{\hbar\omega_\lambda}{k_B T}\right)\right]\right\}. \tag{17}$$

$E(N-1, 1, a_0)$ is the energy of a supercell for the fixed lattice constant a_0, containing $N-1$ atoms and one vacancy, and $E(N, 0, a_0)$ is the energy of the perfect supercell at the same a_0 with N atoms. The enormous advantage of equations (13), (14) is that they require only calculations for one lattice constant $a_0(T = 0)$. Finally, the vacancy formation volume $\Omega_{1V}^{f}(T = 0, p)$ at a given pressure and zero temperature may be obtained by calculating the energies of the supercell with a vacancy and of the perfect supercell as functions of the supercell volume and determining the respective equilibrium volumes V' and V from $p = -\partial E/\partial V$, which yields $\Omega_{1V}^{f}(T = 0, p) = V'(p) - V(p) + \Omega_0$. The vacancy formation energy then is given by

$$E_{1V}^{f}(T = 0, p) = E(N-1, 1, a_0'(p)) - E(N, 0, a_0(p)) + \frac{1}{N}E(N, 0, a_0(p)) \tag{18}$$

where $a_0'(p)$ and $a_0(p)$ are the lattice constants corresponding to $V'(p)$ and $V(p)$. Obviously, equations (13), (18) yield slightly different results for $T = 0, p = 0$. Evaluating in equation (15) $E(N-1, 1, a_0(p=0))$ around $a_0'(p=0)$ yields

$$E(N-1, 1, a_0') + \left.\frac{\partial E}{\partial a_0}\right|_{a_0'} (a_0 - a_0') = E(N-1, 1, a_0')$$

because

$$\left.\frac{\partial E}{\partial a_0}\right|_{a_0'} = 0.$$

Thus, for $T = p = 0$ we have in linear order $E_{1V}^{f}(0,0) = E_{1V}^{f,flc}$ as given by equation (13), whereas equation (18) is correct to any order of $a_0 - a_0'$.

Accordingly, the vacancy migration energy is given by

$$E_{1V}^{m}(T=0, p) = E^{s}(N-1, 1, a_0^{s}(p)) - E(N-1, 1, a_0'(p)) \tag{19}$$

where according to the transition-state theory E^{s} is the energy of the fully relaxed supercell with the migrating atom in the saddle-point configuration, and $a_0^{s}(p)$ is the lattice constant corresponding to the equilibrium volume $V^{s}(p)$ of the supercell. The migration volume is then obtained from

$$\Omega_{1V}^{m}(T=0, p) = V^{s}(p) - V'(p). \tag{20}$$

Because in the calculations finite supercell sizes are used, the results have to be checked for convergence with respect to the supercell size. For E_{1V}^{f} the effect of the finite supercell size may be estimated because it originates (for reasonably large supercells) in many cases mainly from the energy of elastic interaction between the periodically arranged vacancies. For supercell sizes for which these elastic interaction effects may be obtained by the anisotropic continuum theory, the vacancy formation energy E_{1V}^{f} for isolated defects may be determined from the formation energy $E_{1V}^{f}(L)$ obtained from calculations with finite cubic supercells of linear dimensions L via

$$E_{1V}^{f} = E_{1V}^{f}(L) - \frac{A}{L^3} \tag{21}$$

where A is a fit parameter. For the vacancy formation entropy it is much more difficult to estimate the finite-size effect.

For the calculation of the phonon frequencies $\omega_\lambda = \omega_i(\boldsymbol{q})$, where $\boldsymbol{q}$ denotes the phonon wavevector and i labels the various phonon branches, we apply the direct force-constant method [32–38] within the supercell approach. Thereby, single atoms are displaced in the supercell, and the elements $\phi_{l'k'\beta}^{lk\alpha}$ of the force-constant matrix are calculated from the resulting forces on the surrounding atoms. Here the supercells are labelled by the index l (l'), the basis atoms in the supercells by the index k (k'), and the Cartesian directions by α (β). Then the dynamical matrix is determined from the force-constant matrix and the phonon frequencies are obtained from the eigenvalues of the dynamical matrix. Because in a supercell geometry the total force acting on an atom is given by a superposition of the forces exerted by all the atoms in the neighbouring supercells which are equivalent to the displaced atom in the supercell considered and therefore are simultaneously displaced, the calculated dynamical matrix in general is different from the true dynamical matrix which would be obtained for infinitely large supercells. Therefore the results have to be carefully checked with respect to the supercell size. Finally, because the force constants between two atoms in general will decrease (not necessarily monotonically) with increasing separation of the atoms, the force-constant matrix will be truncated at some nearest-neighbour shell in order to reduce the computational effort,

and the linear dimension of the supercell must be chosen to be larger than two times the truncation radius.

From symmetry arguments, the number of displacements of various atoms required to obtain all the desired elements of the force-constant matrix may be drastically reduced. When we determine the couplings from the minimum possible number of calculations using the symmetry arguments, the invariance of the force-constant matrix with respect to the symmetry operations of the crystal point group is automatically guaranteed. Other invariances, however, may be violated due to numerical inaccuracies and have to be restored afterwards:

(i) Because of the symmetry of the force-constant matrix:

$$\phi^{lk\alpha}_{l'k'\beta} = \phi^{l'k'\beta}_{lk\alpha} \tag{22}$$

resulting from the principle of action = reaction, it should be irrelevant which of the atoms (lk) and $(l'k')$ is displaced for a calculation of the coupling constant, but numerically the results of the two calculations may differ slightly. To avoid this problem, we always perform both types of calculation and obtain the final coupling constants from the arithmetic averages.

(ii) If we displace all atoms by the same vector $\boldsymbol{u}^0$, then the forces on all the atoms must vanish, yielding

$$\sum_{l'k'} \phi^{0k\alpha}_{l'k'\beta} = \phi^{0k\alpha}_{0k\beta} + \sum_{l'k'\neq 0k} \phi^{0k\alpha}_{l'k'\beta} = 0 \tag{23}$$

for all k, α, β, where $\phi^{0k\alpha}_{0k\beta}$ is the self-coupling constant. When performing the truncation approximation, i.e., when setting all couplings to atoms outside the truncation sphere to zero, equation (23) in general will be violated. As a result, the acoustic phonon frequencies at $\boldsymbol{q} = 0$ might be non-zero and imaginary. To restore the validity of equation (23), it is tempting to replace the actually determined $\phi^{0k\alpha}_{0k\beta}$ by the negative of the sum on the right-hand side of equation (23):

$$\phi^{0k\alpha}_{0k\beta} \to -\sum_{l'k'\neq 0k} \phi^{0k\alpha}_{l'k'\beta} = S^{\alpha\beta}_k. \tag{24}$$

The same procedure has to be performed for $\phi^{0k\beta}_{0k\alpha}$, i.e.,

$$\phi^{0k\beta}_{0k\alpha} \to -\sum_{l'k'\neq 0k} \phi^{0k\beta}_{l'k'\alpha} = S^{\beta\alpha}_k. \tag{25}$$

However, because of the truncation approximation, the quantities $S^{\beta\alpha}_k$ and $S^{\alpha\beta}_k$ may be different, and thus the symmetry:

$$\phi^{0k\beta}_{0k\alpha} = \phi^{0k\alpha}_{0k\beta}$$

of the force-constant matrix may be violated when calculating the self-coupling constants via equations (24), (25). To avoid this problem, we scale all couplings

$$\{\phi^{0k\alpha}_{0k\beta}, \phi^{0k\alpha}_{l'k'\beta}\} \qquad \text{or} \qquad \{\phi^{0k\beta}_{0k\alpha}, \phi^{0k\beta}_{l'k'\alpha}\}$$

by a factor $\tilde{S}_k/S^{\alpha\beta}_k$ or $\tilde{S}_k/S^{\beta\alpha}_k$ with $\tilde{S}_k = \frac{1}{2}(S^{\alpha\beta}_k + S^{\beta\alpha}_k)$. Thereby another problem arises because among these two sets of coupling constants there are some pairs of coupling constants $\phi^{0k\alpha}_{l'k'\beta}$ and $\phi^{0k\beta}_{l'k'\alpha}$ which must be identical, and to make sure this is correct, these couplings have to be scaled by both factors. As a result, the two sums appearing in equations (24), (25) calculated from the scaled coupling constants are still not identical, but the whole scaling procedure can be repeated until the sums approach the same value, which then is assigned to $\phi^{0k\alpha}_{0k\beta}$ and $\phi^{0k\beta}_{0k\alpha}$.

(iii) Sluiter *et al* [38] considered further sum rules which have to be fulfilled by the coupling constants in order to guarantee the invariance of the system against rigid-body rotations and the symmetry of the tensor of elastic constants. We refrained from modifying the numerically calculated coupling constants in order to fulfil these additional sum rules, because in the sum rules the distances between the coupled atoms enter and hence the coupling constants between further-distant atoms which are already small and numerically less reliable are given a high weight.

(iv) Finally, the displacements which are given to the atoms to calculate the coupling constants have to be chosen large enough in order to avoid numerical inaccuracies but small enough to be compatible with the harmonic approximation. To correct for anharmonic effects, we perform the calculations for positive and negative displacements of the same magnitude u, and evaluate the forces according to $\frac{1}{2}(F(u) - F(-u))$.

2.3. Ab initio electron theory

The forces are calculated by the *ab initio* density functional theory [39], applying the Hellmann–Feynman theorem [40–43]. Two versions of the density functional theory are used, the approach of Kohn and Sham [44] (KS) where the kinetic energy is calculated numerically exactly via the (very time-consuming) self-consistent solution of one-particle Schrödinger equations, and the orbital-free density functional theory [45, 46] (OF-DFT) where the kinetic energy is approximated by an appropriate functional of the electron density. We used the linear-response Perrot functional [46] for Na and a quadratic response functional [47] for Li and K. Because of this approximation the OF-DFT is less accurate than the KS method, and therefore it so far has been successfully applied only to simple metals, e.g., Li, Na, K, Al. We use the OF-DFT mainly for the sake of testing calculations concerning the investigation of finite-size effects resulting from the use of finite supercell sizes, because this method is computationally much less demanding and therefore much larger supercells can be considered than in the KS approach.

Both in the KS approach and in OF-DFT we use the frozen-core approximation and replace the real effective potential of the ionic core by a pseudopotential (see, for instance, reference [42]). In the KS approach we apply norm-conserving non-local *ab initio* pseudopotentials constructed following Vanderbilt [48], including the partial-core correction [49], and we evaluate the crystal wavefunction from plane waves. In OF-DFT we use local pseudopotentials. For Na we apply the empirical pseudopotentials of Topp and Hopfield [50], with the consequence that the calculations for Na cannot be denoted as *ab initio* calculations. For Li and K we use the local pseudopotentials constructed from *ab initio* pseudopotentials (including the partial-core correction for the case of K) according to reference [51].

Because the calculation, especially that of the coupling constants, is numerically rather delicate, the convergence of the results with respect to all the convergence parameters of the methods (e.g., the cut-off energy E_c characterizing the number of plane waves, or the number of k-points used for the sampling of the Brillouin zone) has to be tested very carefully.

3. Cohesive properties

Table 1 shows the theoretical results for the equilibrium lattice constant and the bulk modulus at zero temperature, in comparison with experimental data. The KS calculations yield the well-known overbinding of the local-density approximation, i.e., a slightly too small lattice constant and a slightly too large bulk modulus. Please note also the differences of the results from the KS calculation and the OF-DFT for the lattice constants which probably arise not just from

Table 1. Theoretical results for the equilibrium lattice constant a_0 (in atomic units, au) and the bulk modulus B at zero temperature. The experimental value for B of ^{7}Li was extrapolated from data above 100 K to 0 K.

	a_0 (au)			B (GPa)	
	KS	OF-DFT	Experiments	KS	Experiments
Li	6.34	6.72	6.57 [52] (20 K)	15.2	12.95 [55]
Na	7.65	8.15	8.00 [54] (78 K)	9.1	7.29 [53] (78 K)
K	9.57	9.60	9.88 [54] (5 K)	4.5	3.783 [56] (4.2 K)

the *ansatz* for the kinetic energy of the OF-DFT but also from the different pseudopotentials used for the KS approach and for the OF-DFT.

4. Formation and migration energies and volumes

The alkali metals are often perceived as being among the simplest nearly free-electron metals (which seems to be justified for Na and K but definitely not for Li). Therefore many calculations of the vacancy formation energies used semiempirical approaches starting from the free-electron gas; for a critical review see [57]. Whereas these calculations significantly contributed to a better qualitative understanding of the defect energetics, the quantitative results depend sensitively on the details of the calculations (see tables 1, 2 of [57]). For a reliable calculation of the defect parameters therefore, an *ab initio* calculation is preferable.

The results of the KS calculations for E^{f}, E^{m}, Ω^{f}, and Ω^{m} at zero pressure and temperature obtained in the present paper and in former studies are given in table 2, together with experimental data. The results from the OF-DFT are given in parentheses. For Na there is a good agreement for E^{f} between the data from the KS approach and OF-DFT, whereas for Li there is a considerable discrepancy. Again we want to note that this discrepancy probably does not arise exclusively from the *ansatz* for the kinetic energy of the OF-DFT but also results from the use of different pseudopotentials. There is a good agreement of the KS results with the available experimental data for E^{f} and E^{SD}. Experimentally, it turns out that the Arrhenius plots for the diffusion coefficients (omitting the very low-temperature data of references [13, 14]) are often curved and must be represented by a superposition of two or three exponentials with different activation energies. The quoted values of E^{SD} refer to the respective smallest of these activation energies, and it is often assumed that the corresponding exponential describes the contribution of monovacancies to self-diffusion. For Ω^{SD} the agreement is also reasonable in view of the relatively large error limits of the calculated and probably also of the measured data.

5. Phonon spectra of the ideal crystals

Having in mind the nearly free-electron character of the alkali metals (see section 4), most of the former phonon calculations [59] introduced pseudopotentials for the electron–ion interaction and approximated the electronic response due to an atomic displacement by the one of a homogeneous electron gas. (The linear electronic response of the wavefunction in a realistic crystal potential of Li and K was calculated in reference [60], but this theory contains a

Table 2. Results from the KS formalism and experimental results for the formation energy E^f and the migration energy E^m (in eV), and for the formation volume Ω^f and the migration volume Ω^m at zero pressure and zero temperature (in units of the atomic volume Ω_0 of the ideal crystal). The numbers in parentheses denote the results from the OF-DFT. The estimated error limits for the KS calculations are ± 0.02 eV or ± 0.01 eV for E^f or E^m, and $\pm 0.05\ \Omega_0$ for Ω^f and Ω^m.

		Li	Na	K
E^f	Theory	0.53	0.34 [5]	0.30
		(0.32)	(0.32)	
	Experiment	—	0.354, 0.36 [3]	—
E^m	Theory	0.055 [7]	0.054 [10]	0.051
			(0.026)	
	Experiment	—	—	—
E^{SD}	Theory	0.585	0.394	0.351
			(0.346)	
	Experiment	0.60 [9]	0.391 [14]	0.386 [58]
Ω^f	Theory	0.53	0.5 [18]	0.45
		(0.49)	(0.47)	
	Experiment	—	—	—
Ω^m	Theory	−0.2 [18]	−0.01 [18]	—
			(0.00)	
	Experiment	—	—	—
Ω^{SD}	Theory	0.33	0.49	—
			(0.47)	
	Experiment	0.28 [19]	0.32 [12]	—

certain number of parameters (three for Li and seven for K) which were adjusted by a fit of calculated phonon frequencies to experimental ones). In most of these papers the influence of the various assumptions entering this type of theory is discussed extensively. Because the results sometimes depend critically on the assumptions, an *ab initio* approach is desirable.

In reference [32] we reported the phonon spectra of ideal Li, Na, and K crystals calculated by the same *ab initio* procedure as is used in the present paper (direct force-constant method, supercell approach, KS formalism, *ab initio* pseudopotentials). Most elements of the force-constant matrix were calculated with a cubic supercell containing 54 atoms, apart from the transverse couplings to the atoms in the fourth-nearest-neighbour shell which vanish in a 54-atom supercell and which therefore were determined with an elongated 16-atom supercell. The calculations were performed for the zero-temperature equilibrium lattice constants of the *ab initio* calculations which are smaller than the experimental lattice constants. Apart from a constant scale factor for each material, there was a very good agreement between theoretical and experimental data for the dispersion curves.

In the present paper we report on analogous calculations at the experimental lattice constants of the temperatures for which the phonon spectra were obtained experimentally. Furthermore, we again discuss the finite-size effects by also performing calculations for a 128-atom supercell. Unlike in [32], we did not determine those couplings which are zero for a specific supercell because of symmetry arguments by another type of supercell calculation (for instance, the elongated 16-atom supercell), but we kept the value of zero for them.

For Li we again obtained a good agreement with the experimental data when we performed the calculations for a 54-atom supercell including all couplings up to the fifth-nearest-neighbour shell. When a 128-atom supercell was used with the same range of couplings the results

changed a bit, indicating the finite-size effect for those couplings. However, the results deteriorated when we included the couplings to the eighth-nearest-neighbour shell or all couplings which fit into the supercell, and we then obtained imaginary frequencies near the Γ point (figure 1, to be compared with figure 1 of reference [32] for the results for a 54-atom supercell). To clarify the reason for this, we performed frozen-phonon calculations [32] for some phonon wavelengths. The advantage of such a frozen-phonon calculation is that it includes all couplings up to infinity, i.e., no finite-size effects appear. From these calculations we found no indications for imaginary frequencies near the Γ point. This means that the imaginary frequencies obtained by the direct force-constant method are not due to a failure of the local-density approximation but due to the finite-size effect. According to our calculations the coupling constants in Li decrease considerably more slowly with increasing separation of the atoms than for Na or K, and therefore the finite-size effect is more important. We found that for Na and K the results for the coupling constants from the KS approach and OF-DFT agreed quite well, whereas for Li the coupling strengths obtained by the OF-DFT decease more rapidly than those from the more accurate KS calculations. This in turn means that we cannot use the OF-DFT to estimate the residual finite-size effects in Li by performing calculations for supercells with more than 128 atoms. Altogether, we must conclude that in Li there are far-reaching couplings and that therefore calculations for supercells with far more than 128 atoms

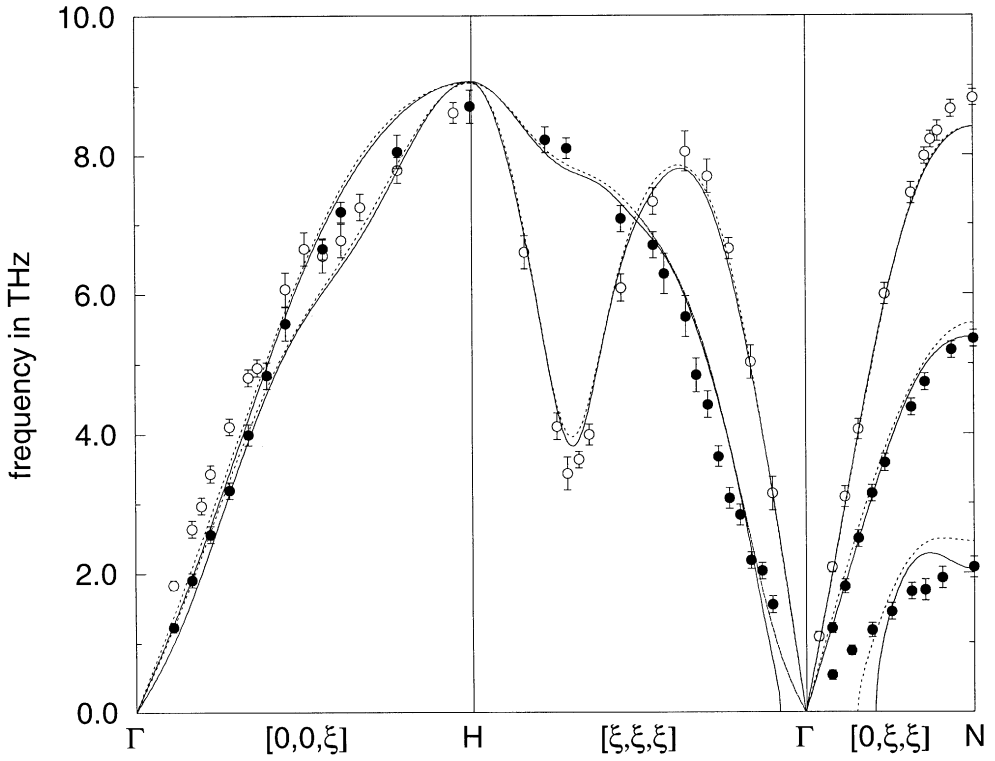

Figure 1. Phonon dispersion curves for bcc Li as calculated by the KS formalism ($E_c = 8.5$ Ryd) for a 128-atom supercell at the experimental lattice constant at $T = 293$ K, $a_0 = 6.634$ au [61]. Couplings up to the eighth-nearest-neighbour shell (dotted lines) and all couplings which fit in the supercell (full lines) are included. The data are compared with results from inelastic neutron scattering [61] at $T = 293$ K (○: longitudinal branches; ●: transverse branches).

would be required for a reliable calculation of the phonon dispersion curves. The previously performed calculations with 54-atom supercells (figure 1 of [32]) yielded reasonable results as compared to the data from inelastic neutron scattering, but the results become worse when including more couplings.

The situation is simpler for the case of Na and K, where the coupling strengths decrease more quickly with increasing distance and where the results from the KS approach and OF-DFT agree much better, with the result that the OF-DFT can be used to estimate the finite-size effects. (The KS calculations for Na and K are much more time consuming than those for Li because of the larger lattice constants which require more plane waves in the basis set for a given E_c.) Figures 2 and 4 exhibit the results for Na and K obtained by the KS formalism for a 54-atom supercell including the couplings up to the fifth-nearest-neighbour shell at the experimental lattice constant and at the temperatures of the respective inelastic neutron scattering experiments [62, 63] and at the zero-temperature *ab initio* lattice constant. Whereas the frequencies for the *ab initio* constant are too large and those for the experimental lattice constant are too small, the form of the dispersion curves varies only slightly with varying lattice constant, and the calculation is able to reproduce the phonon dispersions quite well apart from a constant scale factor (see also reference [32]). With the OF-DFT we obtained only slight changes when going from a 54-atom supercell to a 128-atom supercell, i.e., the results from

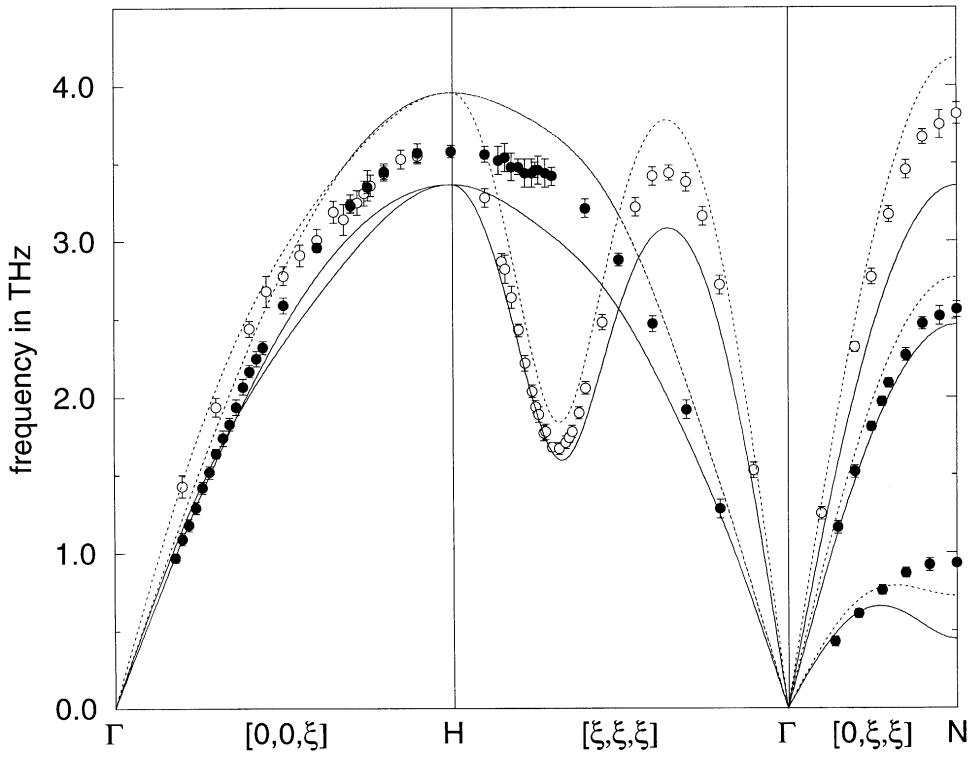

Figure 2. Phonon dispersion curves for bcc Na as calculated by the KS formalism ($E_c = 8.5$ Ryd) for a 54-atom supercell including the couplings up to the fifth-nearest-neighbour shell, for calculations at the experimental lattice constant (full lines) at $T = 90$ K, $a_0 = 7.99$ au [62], and at the zero-temperature *ab initio* lattice constant (dashed lines), in comparison with data from inelastic neutron scattering [62] at $T = 90$ K (○: longitudinal branches; •: transverse branches).

the 54-atom supercell are already well converged with respect to the supercell size. Figures 3 and 5 show that there is a very good agreement between theory and experiment for Na and a good agreement for K when applying the OF-DFT for a 128-atom supercell at the respective experimental lattice constants. Table 3 presents the results for the coupling constants $\phi_{N\alpha\beta}$ of a given atom in the Nth-nearest-neighbour shell. The table records all coupling constants which are non-zero for symmetry reasons and which can be determined in the 54-atom supercell used for the calculations. The theoretical results are compared with the Born–von Kármán couplings which are obtained by fitting an as small as possible number of such parameters to the experimental data [62, 63]. We do not present the data for Li because they are spoiled by the above-discussed finite-size effects.

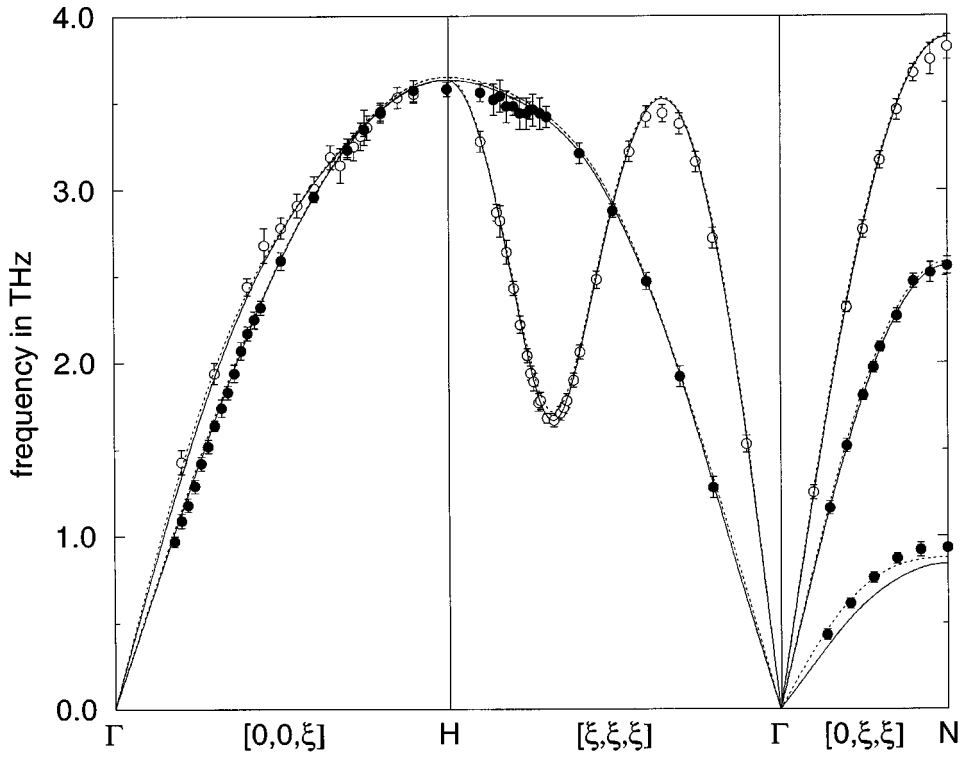

Figure 3. Phonon dispersion curves for bcc Na as calculated by the OF-DFT at the experimental lattice constant at $T = 90$ K, $a_0 = 7.99$ au [62], for a 128-atom supercell including the couplings up to the fifth-nearest-neighbour shell (dotted lines) or all couplings which fit into the supercell (full lines). The data are compared with results from inelastic neutron scattering experiments [62] at $T = 90$ K (○: longitudinal branches; ●: transverse branches).

6. The vacancy formation entropy at zero pressure

In this section we calculate the vacancy formation entropy $S_{1V}^{f}(T, p = 0)$ according to equation (14) from the vacancy formation entropy at fixed lattice constant, $S_{1V}^{f,flc}$, according to equations (16), (12). The determination of the phonon frequencies ω_λ for the supercell with a vacancy is much more complicated than for the perfect supercell. In the latter case one displacement of the central atom of the supercell yields all elements of the force-constant

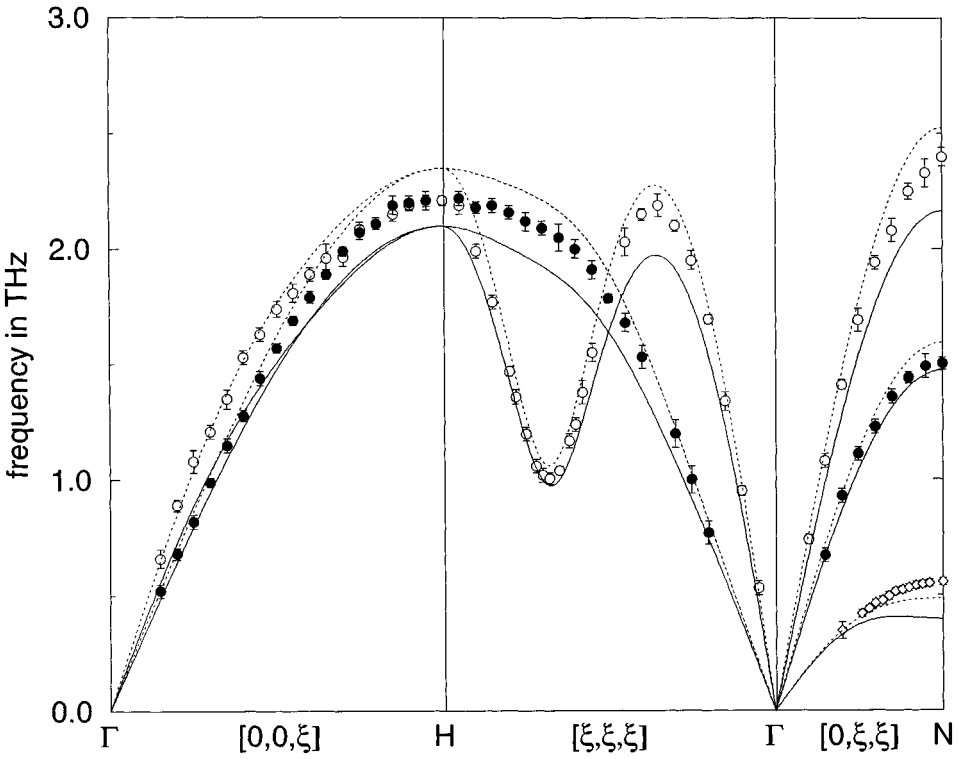

Figure 4. Phonon dispersion curves for bcc K as calculated by the KS formalism ($E_c = 10$ Ryd) for a 54-atom supercell including the couplings up to the fifth-nearest-neighbour shell, for calculations at the experimental lattice constant (full lines) at $T = 9$ K [63], $a_0 = 9.87$ au, and at the zero-temperature *ab initio* lattice constant (dashed lines), in comparison with data from inelastic neutron scattering [63] at $T = 9$ K (○: longitudinal branches; •: transverse branches).

matrix for symmetry reasons [32], whereas for the supercell with a vacancy 17 different atom displacements are required. Furthermore, the configurations with the displaced atoms are of low symmetry and therefore the electronic structure calculation is more demanding.

As outlined in section 5 the reliable determination of phonon frequencies for Li with the KS formalism requires supercell sizes (more than 128 atoms) which are beyond our calculational capability. Furthermore, because the OF-DFT yields coupling strengths for Li which decay more rapidly than those from the KS method, we cannot use the former method to study the finite-size effects. We therefore are not able to give reliable results for the vacancy formation entropy for Li, and we confine ourselves to Na and K for which the phonon frequencies of the perfect crystals could be accurately obtained with supercells containing 54 sites by including the couplings up to the fifth-nearest-neighbour shell. As outlined in section 5, the form of the dispersion curves of these materials varies only slightly with varying lattice constant. From equations (16), (17) the high-temperature limit of the formation entropy can be obtained, yielding $S_{1V}^{f,flc} = -k_B \sum_\lambda \ln(\omega'_\lambda/\omega_\lambda)$, where ω'_λ and ω_λ denote the phonon frequencies in the system with and without vacancies, and therefore a constant scale factor for the frequencies which keeps the form of the dispersion curves invariant drops out and does not influence the high-temperature limit of the formation entropy. All calculations were performed at the lattice constants as obtained by the KS formalism (table 1).

Table 3. Results for the coupling constants $\phi_{N\alpha\beta}$ (in N m^{-1}) of Na and K as obtained from a KS supercell calculation with 54 atoms at the experimental lattice constant, in comparison with Born–von Kármán couplings fitted to the experimental phonon dispersion curves [62, 63].

	Na		K	
$\phi_{N\alpha\beta}$	Theory	Experiment	Theory	Experiment
1 xx	1.017	1.178	0.680	0.7688
1 xy	1.034	1.132	0.724	0.8805
2 xx	−0.015	0.472	0.170	0.4042
2 yy	0.139	0.104	0.060	0.0296
3 xx	−0.032	−0.038	−0.036	−0.0418
3 xy	−0.031	−0.065	−0.022	−0.0455
3 zz	−0.018	0.000	−0.010	0.0038
4 xx	0.052	0.052	0.025	0.0213
4 yy	−0.001	−0.007	<0.0005	−0.0029
4 yz	0.008	0.003	0.001	0.0030
5 xx	0.020	0.017	0.005	0.0091
5 xy	0.009	0.033	0.004	0.0062
7 xx	0.001	—	−0.002	—
7 zz	0.001	—	<0.0005	—
10 xx	<0.0005	—	<0.0005	—

Table 4 presents the results for Na from the KS formalism (a supercell with 54 sites, all couplings up to fifth-nearest-neighbour shell included, $E_c = 10$ Ryd) for the vibrational entropy of the perfect supercell and the supercell with a vacancy and for the formation entropy $S_{1V}^{f,flc}$. As in the case of Li [7], the formation entropy increases monotonically with increasing temperature and attains a nearly constant high-temperature value (in the case of Na for $T > 100$ K). From test calculations we estimate the error arising from the use of a finite E_c, a finite number of $\boldsymbol{k}$-points for the Brillouin zone sampling, and the finite number of frequencies considered in the sum of equation (17) to be about 0.2 k_B. To obtain the formation entropy $S_{1V}^{f}(T, p = 0)$ from $S_{1V}^{f,flc}(a_0(T = 0), T)$ according to equation (14) we used $\beta_p = 2.06 \times 10^{-4}$ K^{-1} [64] for the high-temperature range, $\kappa_T = 1.09 \times 10^{-10}$ Pa^{-1} according to our KS calculations (table 1), and $\Omega_{1V}^{f} = 0.5\,\Omega_0$ [18], yielding $S_{1V}^{f}(T, p = 0) = S_{1V}^{f,flc}(a_0(T = 0), T) - 2.28\ k_B$ and a high-temperature value of $S_{1V}^{f}(T, p = 0) = 1.36\ k_B$. This value is considerably smaller than the various values obtained from various measurements

Table 4. Results for bcc Na from KS calculations for a supercell with 54 sites for the vibrational entropies $S(54, 0)$ and $S(53, 1)$ of the perfect supercell and the supercell with a vacancy and for S_{1V}^{flc} (all in units of k_B) as a function of temperature T (in K). The melting temperature of Na is 371 K.

T	$S(54, 0)$	$S(53, 1)$	$S_{1V}^{f,flc}$
10	1.158	1.380	0.243
100	142.250	142.954	3.339
200	245.392	244.426	3.578
300	309.287	307.185	3.626
370	342.765	340.057	3.640

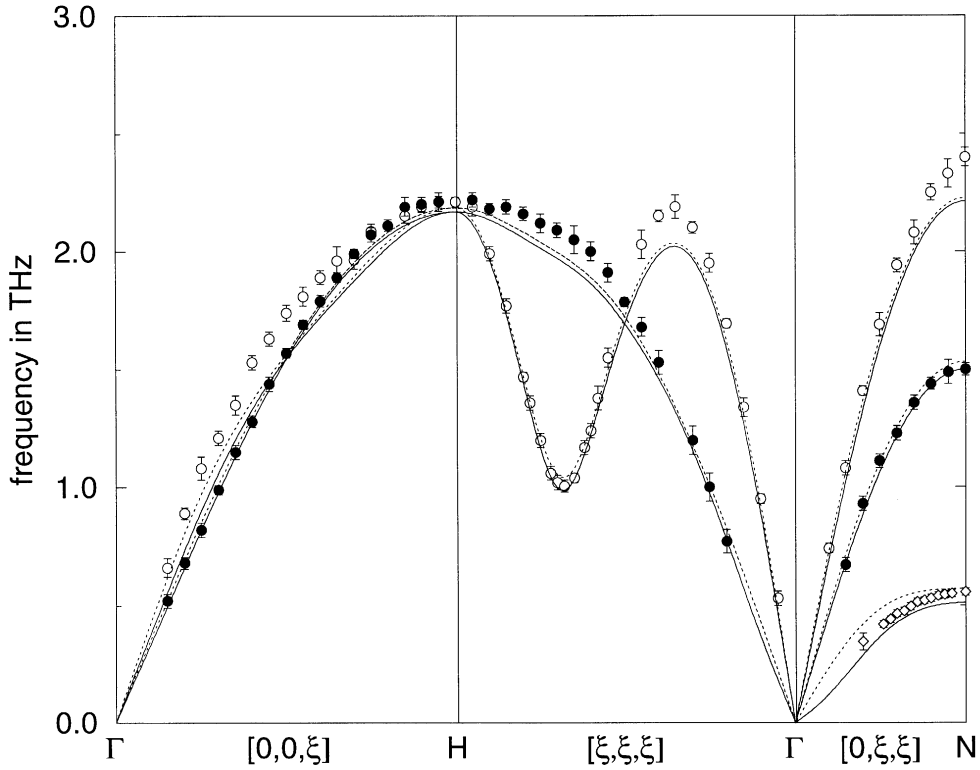

Figure 5. Phonon dispersion curves for bcc K as calculated by the OF-DFT at the experimental lattice constant at $T = 9$ K [63], $a_0 = 9.87$ au, for a 128-atom supercell including couplings up to the fifth-nearest-neighbour shell (dotted lines) or all couplings which fit into the supercell (full lines). The data are compared with results from inelastic neutron scattering experiments [63] at $T = 9$ K (○: longitudinal branches; •: transverse branches).

of the differential thermal expansion when the experimental data are interpreted by assuming only one type of defect ($3.9 \pm 0.7\ k_B \leqslant S_{1V}^{f} \leqslant 5.8 \pm 1.1\ k_B$; for a survey see reference [5]).

To test for residual finite-size effects we performed calculations with the OF-DFT for supercells with 54 atoms and 128 atoms, including the couplings up to the fifth-nearest-neighbour shell. We obtained very similar results (table 5), and we may therefore tentatively assume that the residual finite-size effects are small for Na when using a 54-atom supercell. To illustrate the finite-size effect further we calculated the atom-resolved density of states for

Table 5. Results for $S_{1V}^{f,flc}$ (in k_B) for bcc Na from the OF-DFT for supercells with 54 and 128 sites, as functions of temperature T (in K). The melting temperature of Na is 371 K.

T	$S_{1V}^{f,flc}(54)$	$S_{1V}^{f,flc}(128)$
10	0.579	0.587
100	4.305	4.313
200	4.542	4.564
300	4.589	4.614
370	4.602	4.628

the atoms labelled by k according to

$$n_k(\omega) = \sum_{i,\boldsymbol{q}} \delta(\omega - \omega_i(\boldsymbol{q})) \frac{a_{k,x}^2(\boldsymbol{q},i) + a_{k,y}^2(\boldsymbol{q},i) + a_{k,z}^2(\boldsymbol{q},i)}{|\boldsymbol{a}(\boldsymbol{q},i)|^2}. \tag{26}$$

Here $\boldsymbol{a}(\boldsymbol{q},i)$ is the eigenvector corresponding to the eigenvalue $\omega_\lambda = \omega(\boldsymbol{q},i)$ obtained from the eigenvalue equation for the dynamical matrix. For an isolated vacancy we would expect that the atom-resolved density of states approaches with increasing distance from the vacancy more and more closely to the density-of-states curve for the perfect crystal. It becomes obvious from figure 6 that for the nearest neighbour of the vacancy there are additional low-frequency modes which do not appear in the perfect crystal, whereas the high-frequency peak of the perfect crystal is wiped out. From the second-nearest neighbour to the ninth-nearest neighbour the form of the atom-resolved density of states approaches more and more closely the form of the density-of-states curve for the perfect crystal. In contrast to our expectation the deviations from the perfect crystal become again more pronounced for further-distant atoms and are quite large for the outermost 17th-nearest-neighbour shell. There is one such atom per supercell, which is located in the middle of a cube for which all corner points are occupied by vacancies, i.e., it is connected with the corner points by atom rows along $\langle 111 \rangle$. Due to the structural relaxation around the vacancy (which is strongest along $\langle 111 \rangle$), all atoms in the neighbourhood move away from this atom resulting in a softening of the local modes for this atom as compared to the perfect crystal, and this is definitely a residual finite-size effect.

To illustrate the contributions to the formation entropy from the various neighbour shells of the vacancy we define an atom-resolved vibrational entropy according to

$$S_k = \sum_{i,\boldsymbol{q}} S(\boldsymbol{q},i) \frac{a_{k,x}^2(\boldsymbol{q},i) + a_{k,y}^2(\boldsymbol{q},i) + a_{k,z}^2(\boldsymbol{q},i)}{|\boldsymbol{a}(\boldsymbol{q},i)|^2} \tag{27}$$

where $S_\lambda = S(\boldsymbol{q},i)$ is the contribution of the eigenmode $\lambda = (\boldsymbol{q},i)$ according to equation (17). From S_k the contribution of the whole shell to which atom k belongs is given by $N_k S_k$, where N_k is the number of atoms per supercell in that shell. It is obvious from table 6 that there are considerable contributions to the formation entropy S_{1V}^{f} in addition to that from the nearest-neighbour shell. More than half of the total formation entropy is contributed by further-distant shells. The contribution of the outermost shell is small in spite of the drastically modified atom-resolved density of states. Nevertheless, those shells which do not appear in the supercell with 54 sites (shells 6, 8, 9, 11, 13, 17) contribute $0.763\,k_B$. Because according to table 5 the results for the total S_{1V}^{flc} from the two supercell sizes are rather similar, these additional contributions of the outer shells must be compensated by differences in the contributions of the inner shells for the two supercell sizes. Altogether, this shows that there are still residual finite-size effects for the 54-atom supercell, which—however—approximately compensate each other, so the final result for $S_{1V}^{f,flc}$ appears to be nearly converged with respect to the supercell size.

Table 6. Contributions of the kth-nearest-neighbour shell to $S_{1V}^{f,flc}$ (in units of k_B) in bcc Na as calculated using the OF-DFT for a supercell with 128 sites. The total value of S_{1V}^{flc} is 4.61 k_B.

Shell	1	2	3	4	5	6	7	8	9	10	11	13	17
Contribution to $S_{1V}^{f,flc}$	2.11	−0.39	0.32	0.24	0.64	−0.17	0.53	0.36	0.22	0.42	0.07	0.15	0.11

Table 7 gives the results for $S_{1V}^{f,flc}$ (in units of k_B) for K as obtained from the KS calculation (a supercell with 54 sites, all couplings up to the fifth-nearest-neighbour shell included, $E_c = 10$ Ryd). To obtain the formation entropy $S_{1V}^{f}(T, p = 0)$ from $S_{1V}^{f,flc}(a_0(T = 0), T)$

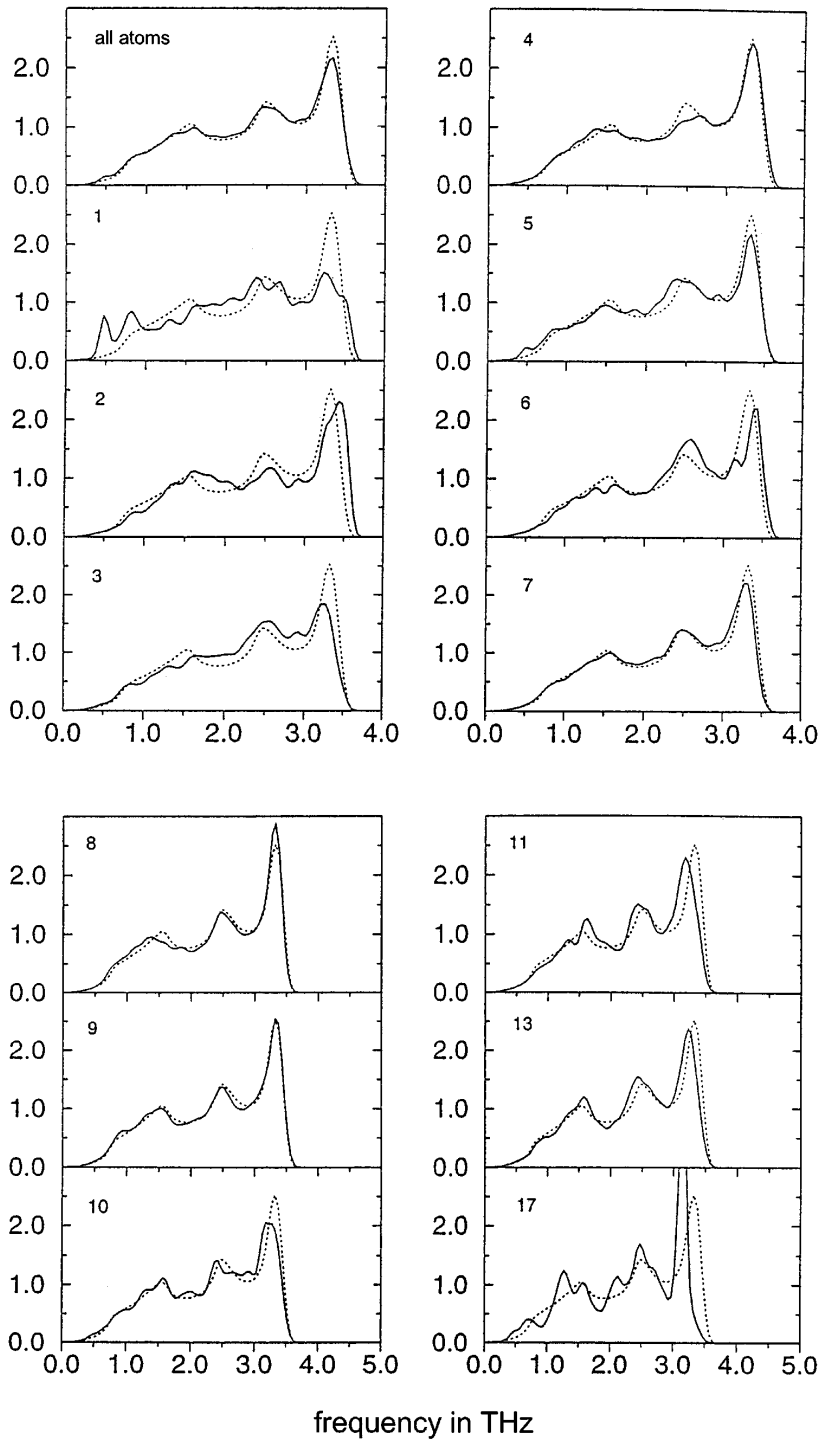

Figure 6. The atom-resolved phonon density of states for atoms of the *k*th-nearest-neighbour shell around a vacancy in Na. The calculations were performed using the OF-DFT for a supercell with 128 sites.

Table 7. Results for $S_{1V}^{f,flc}$ (in units of k_B) for bcc K from KS calculations for a supercell with 54 sites as a function of temperature (in K). The melting temperature of K is 337 K.

T	$S_{1V}^{f,flc}$
10	0.769
100	3.543
200	3.635
300	3.654

according to equation (14), we used $\beta_p = 2.49 \times 10^{-4}$ K^{-1} (at $T \approx 20$ °C [65]), $\kappa_T = (B)^{-1} = (4.5\ \text{GPa})^{-1}$ according to our KS calculations (table 1), and $\Omega_{1V}^f = 0.45\ \Omega_0$ from our KS calculations (table 2), yielding a high-temperature value of $S_{1V}^f(T, p = 0) = 0.78\ k_B$.

7. The self-diffusion coefficient at zero pressure

In this section we calculate the self-diffusion coefficient $D(T)$ for self-diffusion via monovacancies according to equations (6), (7), assuming that the vacancy migration entropy is zero and inserting Flynn's *ansatz* for the attempt frequency, $\nu_0 = \sqrt{3/5}\nu_{\text{Debye}}$. Inserting the Debye frequencies $\nu_{\text{Debye}} = 3.7$ THz [62] for Na and 2.1 THz for K [63] we obtained from our KS calculations

$$D(T, \text{Na}) = 1.32 \times 10^{-2}\ \text{cm}^2\ \text{s}^{-1}\ \exp\left(-\frac{4526\ \text{K}}{T}\right) \tag{28}$$

$$D(T, \text{K}) = 6.5 \times 10^{-3}\ \text{cm}^2\ \text{s}^{-1}\ \exp\left(-\frac{4026\ \text{K}}{T}\right). \tag{29}$$

In figure 7 our theoretical results for bcc Na are compared with the experimental data from radiotracer experiments [12], and there is an excellent agreement for the low-temperature

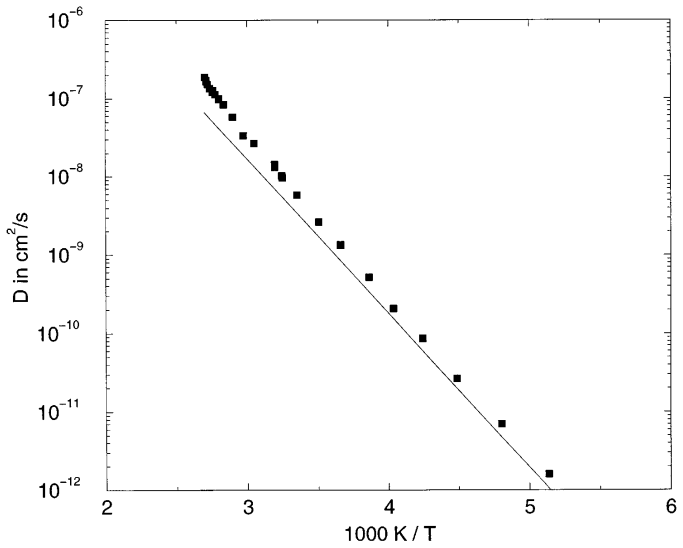

Figure 7. Comparison of our calculated self-diffusion coefficient for bcc Na from the KS formalism (full line) with the experimental data from radiotracer experiments [12].

range, where it is commonly assumed that monovacancies dominate the self-diffusion. The agreement holds both for the slope of the plot of $\ln D$ versus $1/T$, i.e., for the activation energy E^{SD} for self-diffusion, and for the absolute values. For K (figure 8) our absolute values for $D(T)$ are smaller than the experimental values. Fitting the experimental data with one exponential yields [58] $E^{\mathrm{SD}} = 0.406$ eV, whereas fitting with two exponentials yields [58] for the process with the lower activation energy a value of $E^{\mathrm{SD}} = 0.386$ eV, both values being larger than our calculated value of $E^{\mathrm{SD}} = 0.351$ eV.

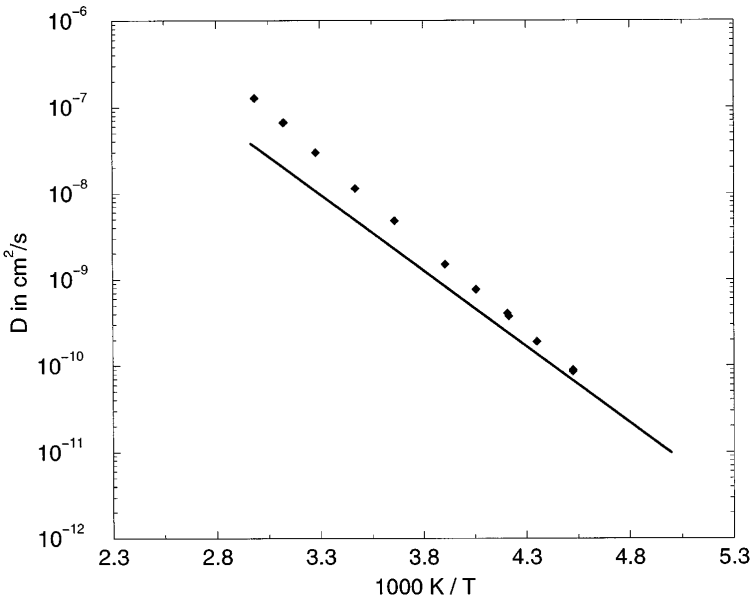

Figure 8. Comparison of our calculated self-diffusion coefficient for bcc K from the KS formalism (full line) with the experimental data from radiotracer experiments [58].

For Li we did not obtain a reliable result for $S^{\mathrm{f}}_{1\mathrm{V}}$ (section 6) and we therefore do not present our data for $D(T)$. The calculated activation energy for self-diffusion via monovacancies is in good agreement with the experimentally obtained activation energy; see table 2.

8. Formation entropy and volume at finite pressure

For the case of Na we calculated by means of the OF-DFT for a supercell with 54 sites using equations (8)–(10) the free enthalpy of vacancy formation $G^{\mathrm{f}}_{1\mathrm{V}}(T, p)$ and then $S^{\mathrm{f}}_{1\mathrm{V}}(T, p) = -\partial G^{\mathrm{f}}_{1\mathrm{V}}/\partial T$ (figure 9) and $\Omega^{\mathrm{f}}_{1\mathrm{V}}(T, p) = \partial G^{\mathrm{f}}_{1\mathrm{V}}/\partial p$ (figure 10). The vacancy formation entropy decreases to zero for zero temperature, but it depends only slightly on the pressure, and therefore the contribution of $\partial S^{\mathrm{f}}_{1\mathrm{V}}/\partial p$ to the formation volume is very small, in contrast to our former conjecture [18]—see also point (iv) of the introduction—and in contrast to the behaviour of ionic crystals. In contrast, the vacancy formation volume is nearly independent of the temperature, but it strongly decreases with increasing pressure: at $T = 0$ K it decreases from $0.43\ \Omega_0$ at $p = 0$ to $0.30\ \Omega_0$ at $p = 2$ GPa. (Close to the melting temperature, $\Omega^{\mathrm{f}}_{1\mathrm{V}}$ decreases even more strongly and attains the value of $0.25\ \Omega_0$ at 2 GPa.) This agrees well with our former KS calculations at zero temperature [18] which found a decrease from $0.5\ \Omega_0$ at $p = 0$ to $0.29\ \Omega_0$ at $p = 2.8$ GPa, and it is also at least qualitatively in line with the experimental observation (point (iv) of the introduction).

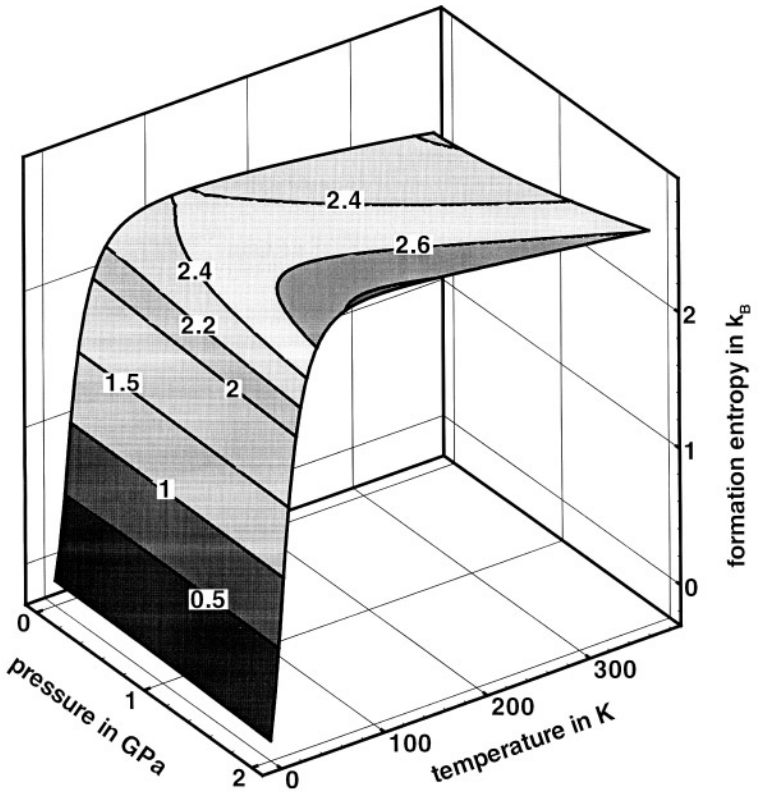

Figure 9. $S^{\mathrm{f}}_{1\mathrm{V}}(T, p)$ for bcc Na as calculated using the OF-DFT. The contour lines are those for constant $S^{\mathrm{f}}_{1\mathrm{V}}$.

9. Summary and conclusions

We calculated, by means of a combination of the *ab initio* electron theory in a supercell approach with the transition-state theory, the defect formation and migration parameters and the diffusion coefficients for self-diffusion via monovacancies for bcc Li, Na, and K. Therein the following assumptions and approximations were made:

(1) The formation entropies were calculated in the harmonic approximation. Because the vacancy migration energies are very small we can imagine that the lattice vibrations become anharmonic for certain directions with a softer potential well than assumed in the harmonic approximation and that this may increase the formation entropies.
(2) We assume that the results for the total vacancy formation entropy of Na and K are well converged with respect to the supercell size, although the single contributions of the various neighbour shells are not yet totally converged.
(3) We assume the validity of the transition-state theory for the calculation of the defect migration parameters in spite of the low migration energies (see point (ii) of the introduction).
(4) The migration entropy is neglected.
(5) We insert Flynn's *ansatz* $\nu_0 = \sqrt{3/5}\nu_{\mathrm{Debye}}$ for the attempt frequency ν_0, which is an open parameter in the transition-state theory.

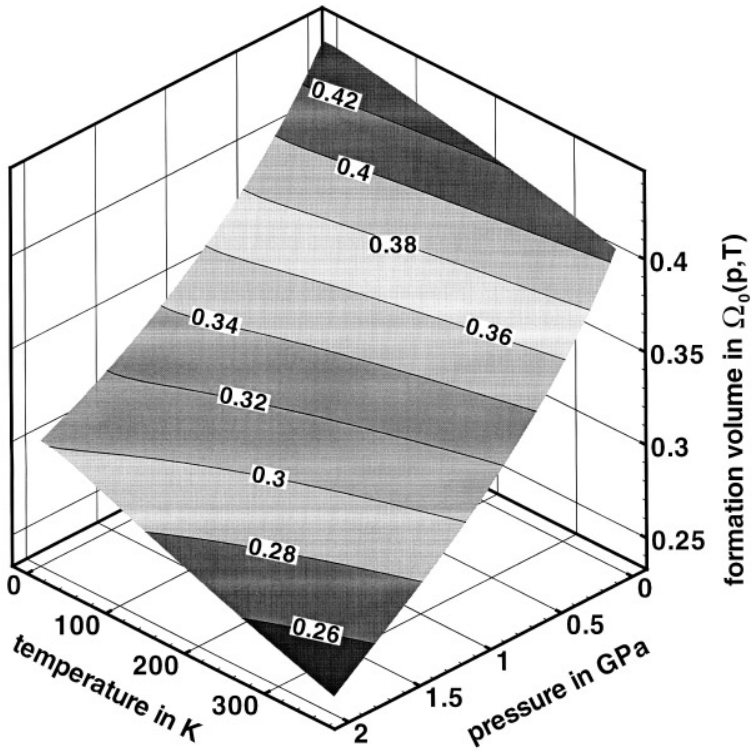

Figure 10. $\Omega^{\mathrm{f}}_{1\mathrm{V}}(T, p)$ for bcc Na as calculated using the OF-DFT. The contour lines are those for constant $\Omega^{\mathrm{f}}_{1\mathrm{V}}(T, p)$.

The following results were obtained:

(a) The vacancy formation energies are 0.53, 0.34, and 0.30 eV for Li, Na, and K with an estimated numerical uncertainty of ± 0.02 eV. Reliable experimental values are only available for Na and are in good agreement with the theoretical result.

(b) The migration energies are about 0.05 eV for all three materials with an estimated numerical uncertainty of ± 0.01 eV.

(c) The calculated activation energies for self-diffusion via monovacancies are 0.585, 0.394, and 0.351 eV with an estimated numerical uncertainty of ± 0.03 eV. They agree well with the experimental data for the contribution of the self-diffusion mechanism with the lowest activation energy (excluding the data at very low temperatures—see point (i) of the introduction).

(d) The calculated formation entropies at high temperatures are 1.36 and 0.78 k_{B} for Na and K, values which are considerably smaller than the formation entropies obtained for Na by measurements of the differential thermal expansion ($3.9 \pm 0.7\ k_{\mathrm{B}} \leqslant S^{\mathrm{f}}_{1\mathrm{V}} \leqslant 5.8 \pm 1.1\ k_{\mathrm{B}}$). Because of points (1), (2) of this section, it is very hard to estimate the numerical uncertainty of our calculated results, but we are convinced that the converged value for Na which would be obtained from a calculation with a very large supercell would be considerably smaller than the experimental values.

(e) For Na the absolute values of the diffusion coefficient as a function of temperature agree well with experimental data from radiotracer experiments. For K our calculated

values are smaller than the experimental values, except for low temperatures. It remains to be investigated whether the deviations at high temperatures can be attributed to the contribution of another mechanism.

(f) The formation volumes are about $0.5\,\Omega_0$ for all three materials with an estimated numerical uncertainty of $\pm 0.05\,\Omega_0$.

(g) The migration volumes are -0.2 and $-0.01\,\Omega_0$ for Li and Na with an estimated numerical uncertainty of $\pm 0.05\,\Omega_0$. The systematic error arising from the application of the transition-state theory in spite of the low vacancy migration energy cannot be estimated.

(h) The activation volumes at zero pressure are 0.33 and $0.49\,\Omega_0$ for Li and Na. In view of the large uncertainties for the theoretical and the experimental determination, the agreement with the experimental values is satisfactory.

(i) The formation entropy of Na depends only slightly on pressure, and thus there is only a very small contribution of $\partial S^{\mathrm{f}}_{1\mathrm{V}}/\partial p$ to the formation volume, in contrast to a former conjecture (see point (iv) of the introduction).

(k) The formation volume decreases strongly with increasing pressure in at least qualitative agreement with the experiments (see point (iv) of the introduction).

To summarize, there is a good agreement of our calculated results for monovacancies with available experimental data for the formation and activation parameters at intermediate temperatures, except for the formation entropy. For this quantity the theory yields considerably smaller values than expected from the experimental data for Na, but it must be kept in mind that it is extremely difficult to determine this parameter both theoretically (see points (1), (2)) and experimentally (as becomes obvious from the large scatter of experimental data). Altogether, there seems to be no doubt that monovacancies provide the dominant contribution to the self-diffusion in Li, Na, and K at intermediate temperatures.

References

[1] Feder R 1970 *Phys. Rev.* B **2** 828
[2] Feder R and Charbnau H P 1966 *Phys. Rev.* **149** 464
[3] Adlhart W, Fritsch G and Lüscher E 1970 *J. Appl. Phys.* **41** 5071
[4] Frank W, Breier U, Elsässer C and Fähnle M 1993 *Phys. Rev.* B **48** 7676
[5] Breier U, Frank W, Elsässer C, Fähnle M and Seeger A 1994 *Phys. Rev.* B **50** 5928
[6] Göltz G, Heidemann A, Mehrer H, Seeger A and Wolf D 1980 *Phil. Mag.* A **41** 723
[7] Frank W, Breier U, Elsässer C and Fähnle M 1996 *Phys. Rev. Lett.* **77** 518
[8] Lodding A, Mundy J N and Ott A 1970 *Phys. Status Solidi* **38** 559
[9] Feinauer A 1993 *PhD Thesis* University of Stuttgart, p 68
[10] Breier U 1996 *PhD Thesis* University of Stuttgart
[11] Brünger G, Kanert O and Wolf D 1980 *Phys. Rev.* B **22** 4247
[12] Mundy J N 1971 *Phys. Rev.* B **3** 2431
[13] Wieland O 1999 *PhD Thesis* University of Stuttgart
[14] Neumann M, Scharwaechter P, Seeger A, Frank W, Freitag K, Konuma M and Majer G 1997 *Defect Diffusion Forum* **143–147** 85
[15] Seeger A 1993 *Defect Diffusion Forum* **95–98** 147
[16] Vineyard G H 1957 *J. Phys. Chem. Solids* **3** 121
[17] Schott V, Fähnle M and Seeger A 1997 *Phys. Rev.* B **56** 7771
[18] Breier U, Schott V and Fähnle M 1997 *Phys. Rev.* B **55** 5772
[19] Hultsch R A and Barnes R G 1962 *Phys. Rev.* **125** 1832
[20] Bertani R, Mali M, Roos J and Brinkmann D 1990 *J. Phys.: Condens. Matter* **2** 7911
[21] Kluthe S 1994 *PhD Thesis* University of Zürich
[22] Brinkmann D, private communication
[23] Biernacki S, Scherz U, Gillert R and Scheffler M 1989 *Mater. Sci. Forum* **38–41** 625
[24] Blöchl P E, Smargiassi E, Car R, Laks D B, Andreoni W and Pantelides S T 1993 *Phys. Rev. Lett.* **70** 2435

[25] Smargiassi E and Madden P A 1995 *Phys. Rev.* B **51** 129
[26] Flynn C P 1972 *Point Defects and Diffusion* (Oxford: Clarendon)
[27] Wallace D 1972 *Thermodynamics of Crystals* (Chichester: Wiley)
[28] Satta A, Willaime F and de Gironcoli S 1998 *Phys. Rev.* B **57** 11 184
[29] Gillan M J 1981 *Phil. Mag.* A **43** 301
[30] Harding J H 1985 *Physica* B **131** 13
[31] Catlow C R A, Corish J, Jacobs P W M and Lidiard A B 1981 *J. Phys. C: Solid State Phys.* **14** L121
[32] Frank W, Elsässer C and Fähnle M 1995 *Phys. Rev. Lett.* **74** 1791
[33] Kunc K and Martin R M 1982 *Phys. Rev. Lett.* **48** 406
[34] Kresse G, Furthmüller J and Hafner J 1995 *Europhys. Lett.* **32** 729
[35] Parlinski K, Li Z Q and Kawazoe Y 1997 *Phys. Rev. Lett.* **78** 4063
[36] Meyer B, Schott V and Fähnle M 1998 *Phys. Rev.* B **58** R14 673
[37] Heid R, Bohnen K-P and Ho K M 1998 *Phys. Rev.* B **57** 7407
[38] Sluiter M H, Weinert M and Kawazoe Y 1999 *Phys. Rev.* B **59** 4100
[39] Hohenberg P and Kohn W 1964 *Phys. Rev.* **136** B804
[40] Hellmann H 1937 *Einführung in die Quantenchemie* (Leipzig: Deuticke)
[41] Feynman R P 1939 *Phys. Rev.* **56** 340
[42] Ihm J, Zunger A and Cohen M L 1979 *J. Phys. C: Solid State Phys.* **12** 4409
[43] Fähnle M, Elsässer C and Krimmel H 1995 *Phys. Status Solidi* b **191** 9
[44] Kohn W and Sham L J 1965 *Phys. Rev.* **140** A1133
[45] Pearson M, Smargiassi E and Madden P A 1993 *J. Phys.: Condens. Matter* **5** 3221
[46] Smargiassi E and Madden P A 1994 *Phys. Rev.* B **49** 5220
[47] Foley M and Madden P A 1996 *Phys. Rev.* B **53** 10 589
[48] Vanderbilt D 1985 *Phys. Rev.* B **32** 8412
[49] Louie S G, Froyen S and Cohen M L 1982 *Phys. Rev.* B **26** 1738
[50] Topp W C and Hopfield J J 1973 *Phys. Rev.* B **7** 1295
[51] Watson S, Jesson B J, Carter E A and Madden P A 1998 *Europhys. Lett.* **41** 37
[52] Berliner R and Werner S A 1986 *Phys. Rev.* B **34** 3586
[53] Diederich M E and Trivisonno J 1966 *J. Phys. Chem. Solids* **27** 637
[54] Barrett C S 1956 *Acta Crystallogr.* **9** 671
[55] Felice R A, Trivisonno J and Schuele D E 1977 *Phys. Rev.* B **16** 5173
[56] Gugan D 1997 *Phys. Scr.* **56** 95
[57] Evans R and Finnis M W 1976 *J. Phys. F: Met. Phys.* **6** 483
[58] Mundy J N, Miller T E and Porte R J 1971 *Phys. Rev.* B **3** 2445
[59] Dagens L, Rasolt M and Taylor R 1975 *Phys. Rev.* B **11** 2726
Hafner J 1976 *Z. Phys.* B **24** 41
Perdew J P and Vosko S H 1978 *J. Phys. F: Met. Phys.* **6** 1421
Day R S, Sun F, Cutler P H and King W F III 1977 *J. Phys. F: Met. Phys.* **7** L169
Falter C, Rakel H and Ludwig W 1988 *Phys. Rev.* B **38** 3986
Singh N and Yadav B S 1993 *Physica* **192** 205
[60] Weilacher K H, Roth-Seefried H and Bross H 1977 *Phys. Status Solidi* b **80** 137
Aviran A, Weilacher K H and Bross H 1978 *Z. Phys.* B **29** 13
[61] Beg M and Nielsen M 1976 *Phys. Rev.* B **14** 4266
[62] Woods A D B, Brockhouse B N, March R H, Stewart A T and Bowers R 1962 *Phys. Rev.* **128** 1112
[63] Cowley R A, Woods A D B and Dolling G 1966 *Phys. Rev.* **150** 487
[64] Corruccini R J 1957 *Chem. Eng. Prog.* **53** 262
Corruccini R J 1957 *Chem. Eng. Prog.* **53** 342
Corruccini R J 1957 *Chem. Eng. Prog.* **53** 397
[65] Mitra S S and Joshi S H 1961 *J. Chem. Phys.* **34** 1462